Cell
P R E S S

The Ankyrin Repeats of TRPV1 Bind Multiple Ligands and Modulate Channel Sensitivity

Polina V. Lishko,[1,2,3] Erik Procko,[1,2] Xiangshu Jin,[1,2,4] Christopher B. Phelps,[1] and Rachelle Gaudet[1,*]

[1] Department of Molecular and Cellular Biology, Harvard University, 7 Divinity Avenue, Cambridge, MA 02138, USA
[2] These authors contributed equally to this work.
[3] Present address: Department of Physiology, University of California San Francisco, Genentech Hall N274, 600 16th Street, San Francisco, CA 94158, USA.
[4] Present address: Department of Biochemistry and Molecular Biophysics, Columbia University, 630 West 168th Street, New York, NY 10032, USA.
*Correspondence: gaudet@mcb.harvard.edu
DOI 10.1016/j.neuron.2007.05.027

SUMMARY

TRPV1 plays a key role in nociception, as it is activated by heat, low pH, and ligands such as capsaicin, leading to a burning pain sensation. We describe the structure of the cytosolic ankyrin repeat domain (ARD) of TRPV1 and identify a multiligand-binding site important in regulating channel sensitivity within the TRPV1-ARD. The structure reveals a binding site that accommodates triphosphate nucleotides such as ATP, and biochemical studies demonstrate that calmodulin binds the same site. Electrophysiology experiments show that either ATP or PIP_2 prevent desensitization to repeated applications of capsaicin, i.e., tachyphylaxis, while calmodulin plays an opposing role and is necessary for tachyphylaxis. Mutations in the TRPV1-ARD binding site eliminate tachyphylaxis. We present a model for the calcium-dependent regulation of TRPV1 via competitive interactions of ATP and calmodulin at the TRPV1-ARD-binding site and discuss its relationship to the C-terminal region previously implicated in interactions with PIP_2 and calmodulin.

INTRODUCTION

The six mammalian TRP channels of the vanilloid subfamily (TRPV) are important in sensory and pain perception and in calcium homeostasis. TRPV1, a nonselective cation channel expressed in peripheral nociceptor sensory neurons, is responsible for sensing noxious heat (>42°C) and transducing inflammatory pain signals (reviewed in Caterina and Julius, 2001 and Tominaga and Tominaga, 2005). At a molecular level, TRPV1 is activated by noxious heat, low extracellular pH (Caterina et al., 1997; Tominaga et al., 1998), and several ligands, including vanilloids such as capsaicin and resiniferatoxin (Caterina et al., 1997).

TRPV1 undergoes two types of desensitization upon activation by capsaicin or protons: acute (short-term) desensitization and tachyphylaxis or loss of sensitivity to repeated stimulations (Koplas et al., 1997). Physiologically, TRPV1 desensitization can lead to adaptation of peripheral neurons to pain perception. The regulatory lipid phosphatidylinositol-4,5-bisphosphate (PIP_2) is a putative intracellular modulator of TRPV1, although there is some debate as to whether it sensitizes or desensitizes the channel. Mutations in a C-terminal cytosolic region of TRPV1 indicate an inhibitory role for PIP_2 (Prescott and Julius, 2003). However, others have found that PIP_2 sensitizes TRPV1 and that depletion leads to desensitization (Liu et al., 2005; Stein et al., 2006). Intracellular ATP can also sensitize TRPV1, although there is controversy about whether it is through a direct interaction (Kwak et al., 2000) or indirectly through PIP_2 synthesis (Liu et al., 2005).

An increase in intracellular calcium concentration causes TRPV1 desensitization, and calmodulin (CaM), a ubiquitous calcium-sensor, may play a role in mediating this effect (Numazaki et al., 2003; Rosenbaum et al., 2004). CaM interacts in vitro with isolated peptides from the TRPV1 N-terminal region in a Ca^{2+}-dependent manner (Rosenbaum et al., 2004), and also binds to the TRPV1 C-terminal region in a Ca^{2+}-independent manner (Numazaki et al., 2003).

TRPV proteins have large N- and C-terminal cytosolic domains and six putative transmembrane segments similar to those of Shaker potassium channels and, by analogy, probably assemble as tetramers. The N-terminal region contains six ankyrin repeats (Jin et al., 2006; McCleverty et al., 2006) which are essential for channel function (Hellwig et al., 2005; Jung et al., 2002). Ankyrin repeats are 33-residue sequence motifs often involved in protein-protein interactions. They are present in many proteins with functions that include signaling, cytoskeleton integrity, transcription, and cellular localization (Mosavi et al., 2004; Sedgwick and Smerdon, 1999). Recently, we and others have determined the structure of the TRPV2 ankyrin repeat domain (ARD) (Jin et al., 2006; McCleverty et al., 2006). A close homolog of TRPV1 (44% sequence identity), TRPV2 is insensitive to capsaicin and activated

Table 1. Data Collection and Refinement Statistics for TRPV1-ARD

	Crystal Form I				Crystal Form II
Data Collection	Crystal 1 Se-Met			Crystal 2	
Space group	P321			P321	R3
Cell dimensions: *a*, *b*, *c* (Å)	124.6, 124.6, 62.8			124.7, 124.7, 62.8	99.5, 99.5, 106.7
	Peak	*Inflection*	*Remote*		
Wavelength	0.97907	0.97922	0.99298	1.5418	1.5418
Resolution (Å)	3.3 (3.42-3.3)	3.4 (3.52-3.4)	3.2 (3.31-3.2)	3.2 (3.31-3.2)	2.7 (2.8-2.7)
R_{sym}	0.082 (0.271)	0.113 (0.550)	0.14 (0.408)	0.091 (0.605)	0.107 (0.569)
$I / \sigma I$	9.8 (4.0)	10.5 (1.9)	5.8 (1.9)	9.1 (1.8)	24.9 (3.1)
Completeness (%)	99.6 (96.3)	99.8 (99.7)	96.0 (98.2)	98.8 (99.9)	100.0 (99.7)
Redundancy	8.8	7.0	2.7	4.5	4.5
Refinement					
Resolution (Å)				20-3.2	20-2.7
No. unique reflections				8450	9618
R_{work}/R_{free}				0.235 / 0.286	0.199 / 0.248
Molecules/a.u.				1	1
Residues in model				110-240, 247-359	111-358
No. atoms					
Protein				1893	1998
Ligand (ATP)				31	31
Water				—	72
B-factors					
Protein				115.3	37.7
Ligand/ion				107.9	53.6
Water					44.9
RMS deviations					
Bond lengths (Å)				0.009	0.012
Bond angles (°)				1.24	1.72

One crystal was used per data set. Values in parentheses are for the highest resolution shell.

at a higher temperature threshold of >52°C (Caterina et al., 1999). The TRPV2-ARD structure comprises six ankyrin repeats. The isolated TRPV2-ARD is monomeric, suggesting that the ARD of TRPV proteins may be used for interactions with regulatory factors rather than in promoting tetrameric channel assembly.

Here we describe the crystal structure of the TRPV1-ARD and the identification of a multiligand-binding site that is important in regulating ion channel sensitivity. Our structure and further mutagenesis demonstrate that CaM and ATP interact at the same site. Using electrophysiology, we show that ATP directly prevents tachyphylaxis to repeated applications of capsaicin, while CaM is necessary for tachyphylaxis. We also provide further evidence that PIP$_2$ sensitizes TRPV1, suggesting ATP acts both directly by binding to the TRPV1-ARD in competition with CaM and indirectly by regenerating depleted PIP$_2$.

RESULTS

Structure of the TRPV1-ARD
The TRPV1-ARD (residues 101–364) produced in *E. coli* behaved as a monomer in solution at concentrations of up to 300 μM, as determined by size exclusion chromatography and multiangle light scattering (data not shown). We determined the structure of the TRPV1-ARD in two crystal forms using a combination of multiwavelength anomalous diffraction and molecular replacement (Table 1). The two structures are essentially identical, with an overall root mean squared deviation (RMSD) of 0.76 Å over 241 Cα atoms, and crystal form II (higher resolution at 2.7 Å) is used for most analyses (Figure 1). The overall TRPV1-ARD fold is very similar to TRPV2-ARD (Figure 1B; RMSD = 1.4 Å over 240 Cα atoms) (Jin et al., 2006; McCleverty et al., 2006), comprising six ankyrin repeats, each
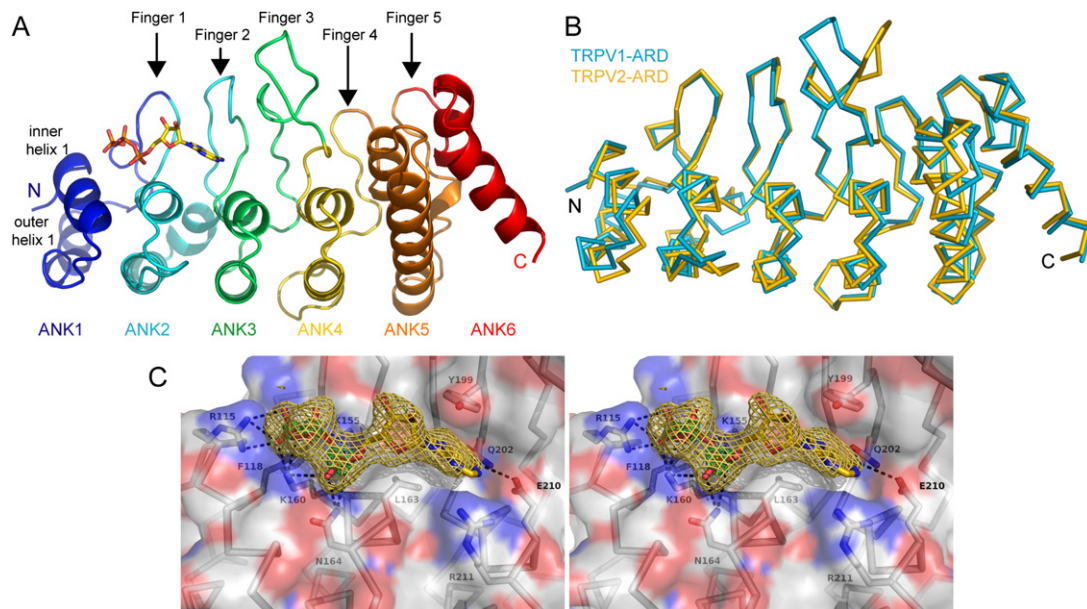
Figure 1. TRPV1-ARD Structure

(A) Ribbon diagram of TRPV1-ARD showing each ankyrin repeat in a distinct color with the bound ATP in stick representation.

(B) Superposition of TRPV1-ARD (cyan) and TRPV2-ARD (gold).

(C) Stereo diagram of residues within 4 Å of the ATP in crystal form II with polar interactions indicated by dashed lines. The final σA-weighted $2F_o - F_c$ map is contoured at 1.5σ (yellow) and 5σ (green) around the ATP.

consisting of a pair of antiparallel α helices followed by a "finger" loop. The concave surface formed by the inner helices and fingers is often a site of protein-protein interactions in other ankyrin repeat proteins (Mosavi et al., 2004; Sedgwick and Smerdon, 1999). As in TRPV2, fingers 1, 2, and 3 and outer helices 5 and 6 are unusually long, and a large counterclockwise twist observed in the stacking of repeats four and five breaks the regularity of the domain.

Despite their overall similarity, there are some notable differences between the TRPV1- and TRPV2-ARD structures. One difference is the conformation of the long finger 3, which is disordered in crystal form I, folded over toward finger 2 in crystal form II, and flexible in TRPV2 (Figure 1B) (Jin et al., 2006). The TRPV1-ARD is significantly more positively charged, with a calculated isoelectric point of 8.3, compared to 5.8 for TRPV2-ARD. This divergence in surface shape and electrostatic properties likely reflects differing biological functions, such as specificity and affinity for distinct interacting partners.

ATP Interacts with a Specific Site on the TRPV1-ARD

A significant feature was not accounted for by protein residues in the electron density maps of both TRPV1-ARD structures. Based on the size and shape of this electron density feature, together with the fact that 5 mM ATP was present in the crystallization solutions, we modeled it as an ATP molecule (Figure 1C). In crystal form I, two ATP molecules bridge the interface between two crystallographically related molecules (see Figure S1 in the Supple-

mental Data available with this article online), while in crystal form II the TRPV1-ARD binds ATP at the same site in the absence of those crystal-packing interactions. The presence of ATP at the same site in both crystal forms suggests that this interaction is specific, independent of crystal lattice formation, and may be physiologically relevant.

The ATP-binding site is formed by the concave surface of repeats 1–3, with positive residues R115 (inner helix 1) and K155 and K160 (inner helix 2) interacting with the triphosphate, while L163 (inner helix 2) and Y199 (finger 2) sandwich the adenine base. The adenine N6 amine also interacts with Q202 (finger 2) and E210 (inner helix 3) (Figure 1C).

To determine whether the interaction of TRPV1-ARD with ATP is also observed biochemically, we used ATP-agarose to pull down purified TRPV1-ARD. The ATP-agarose pulled down TRPV1-ARD but not TRPV2-ARD, and free ATP competed the interaction (Figure 2). Three mutations within the ATP-binding site—K155A and K160A, which interact with the triphosphate moiety, and the double mutation Y199A/Q202A, residues interacting with the adenine base—impaired the TRPV1-ARD interaction with ATP-agarose (Figures 2A and 2B). Furthermore, two distal negative control mutations, R181A (outer helix 2) and K265A (outer helix 4), both on the convex face of TRPV1-ARD, did not impair ATP-agarose binding (Figures 2A and 2B). The mutational data therefore demonstrate that the interaction with ATP is also observed biochemically and requires residues identified in the crystal structure.
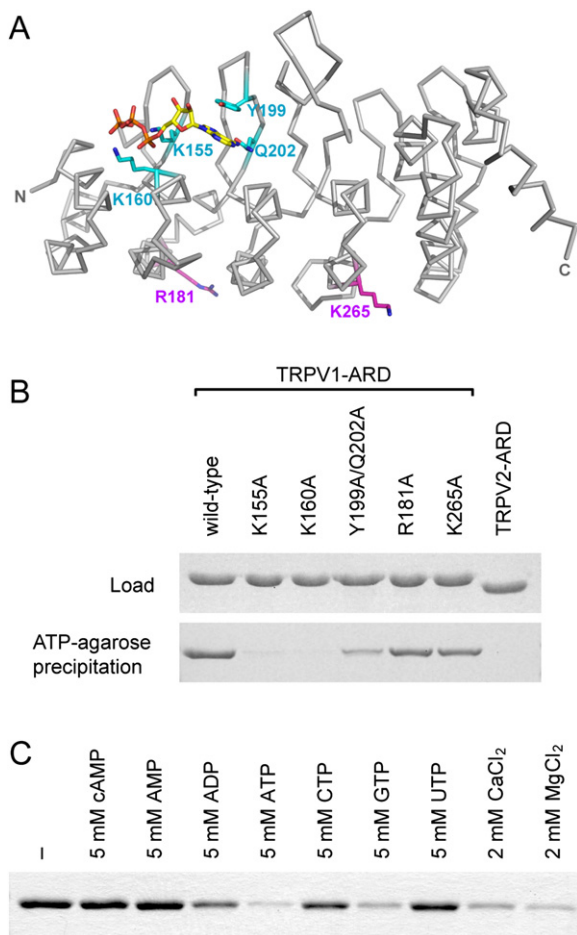
Figure 2. TRPV1-ARD Binds ATP

(A) Cα trace of the TRV1-ARD with ATP (yellow) and the sidechains of the ATP-interacting residues (cyan) and distant negative control residues (magenta) shown as sticks.

(B and C) Coomassie-stained gels show (B) wild-type and mutant TRPV1-ARD proteins loaded (top) and bound (bottom) to ATP-agarose, and (C) wild-type TRPV1-ARD protein bound to ATP-agarose in the presence of the indicated concentration of competing compounds.

To further define the specificity of the identified binding site, we tested whether other nucleotides could successfully compete the ATP-agarose interaction. Incubation with purine triphosphate nucleotides (ATP and GTP; Figure 2C) successfully competed the ATP-agarose pulldown. ADP and the pyrimidine triphosphate nucleotides (CTP and UTP) only partially competed the interaction at the same concentration (5 mM), while AMP and cyclic AMP did not prevent binding to ATP-agarose (Figure 2C). In aggregate, these results indicate that both a purine base and a triphosphate moiety are important for optimal binding to TRPV1-ARD.

Competition experiments also indicated that the divalent cations Mg^{2+} and Ca^{2+}, which are chelated by the triphosphate moiety of ATP, reduce binding of TRPV1-ARD to ATP-agarose (Figure 2C). Although most intracellular

ATP is chelated with Mg^{2+}, the cellular concentration of free ATP is still significant (0.3–0.7 mM; Taylor et al., 1991), and ATP may well be a relevant physiological ligand.

Furthermore, our observation of ATP bound to the concave face of TRPV1-ARD is intriguing in light of previously published data showing upregulation of TRPV1 activation by intracellular ATP (Kwak et al., 2000). Kwak and colleagues likened residues 173–178 in the TRPV1 N terminus to a nucleotide binding Walker B motif based on sequence similarity, and found that a D178N substitution abolished ATP-mediated upregulation (Kwak et al., 2000). Our structure shows that this segment is part of outer helix 2 rather than forming the typical Walker B β strand and is on the face opposite the ATP found in our structure. Furthermore, one of our negative control mutants, R181A, still binds ATP, even though the R181 sidechain is adjacent to D178 in our structure. Overall, the ATP-binding site we observe is unlike that of most known nucleotide triphosphate binding proteins or hydrolases, which have a Walker A or P loop motif (GxxGxGKST where x is any amino acid; Walker et al., 1982) interacting with the nucleotide's α and β phosphates.

Mutations in the ATP-Binding Site of TRPV1 Affect Its Response to Capsaicin

As mentioned above, it has been reported that intracellular ATP modulates TRPV1 desensitization. Kwak and colleagues proposed that TRPV1 binds ATP directly (Kwak et al., 2000). In contrast, Liu and colleagues argued that intracellular ATP is required for resynthesis of PIP_2 (Liu et al., 2005). In their model, PIP_2 is rapidly hydrolyzed upon TRPV1 activation and depletion of the PIP_2 pool in the absence of ATP leads to channel inactivation (Liu et al., 2005).

To test whether the ATP-binding site on the TRPV1-ARD is important for channel function, the mutations that impair ATP binding were introduced into full-length rat TRPV1. We initially characterized the behavior of wild-type rat TRPV1 in baculovirus-infected Sf21 insect cells. In whole-cell patch-clamp electrophysiology experiments, the insect-cell-expressed TRPV1 channel was sensitive to capsaicin and capsazepine, a competitive antagonist of capsaicin, in the same concentration range as TRPV1 expressed endogenously in dorsal root ganglions, or heterologously in HEK293 cells or *Xenopus laevis* oocytes (Figures S2 and S3) (Jordt and Julius, 2002; Voets et al., 2004). Mock-infected insect cells had no endogenous capsaicin-evoked current (Figure S2B).

Repeated capsaicin applications lead to strong tachyphylaxis of TRPV1 current in the absence of ATP in the recording pipette (Figure 3). That is, current responses are nearly eliminated upon repeated applications of capsaicin. Of note, TRPV1 showed faster acute desensitization when expressed in HEK293 cells, compared to insect cells (Figure S3). Adding 4 mM ATP to the recording pipette essentially eliminated tachyphylaxis in insect cells (Figure 3). ATPγS, a nonhydrolyzable analog, also essentially eliminated tachyphylaxis, whereas an alternative
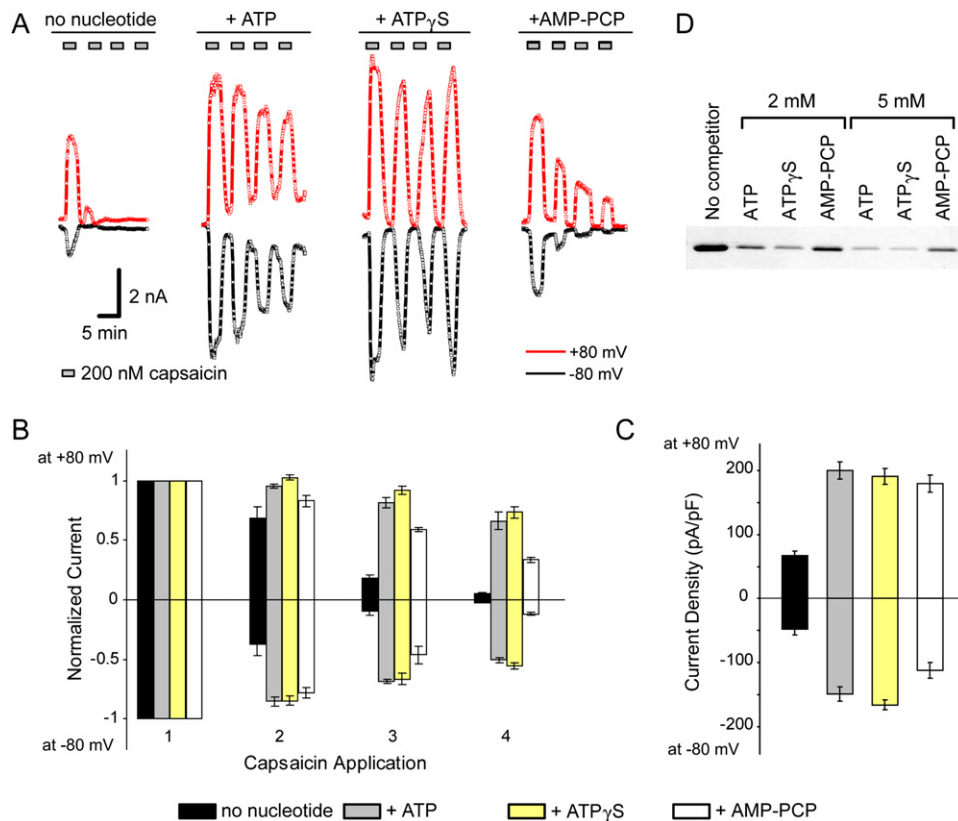
Figure 3. ATP and Nonhydrolyzable Analogs Sensitize TRPV1 and Reduce Tachyphylaxis

(A) Recordings from TRPV1-expressing insect cells in the absence or presence of nucleotide in the recording pipette, as indicated. For the recordings in the presence of nucleotide, 4 mM nucleotide was added to the pipette (intracellular) solution and was therefore present throughout the recording. Cells were repeatedly stimulated with 200 nM capsaicin for 3 min with 3 min washouts. The +80 mV (red) and −80 mV (black) currents are shown, extracted from 1500 ms voltage ramps.

(B and C) Mean current amplitudes for successive capsaicin applications, normalized to the current amplitudes obtained on the first application (B) and mean current density of the maximal response to the first capsaicin application normalized to the cell capacitance (C) in the absence (black) or presence of ATP (gray), ATPγS (yellow), or AMP-PCP (white) (n = 4, 4, 5, and 5 cells, respectively). Error bars are SEM.

(D) Coomassie-stained gel of wild-type TRPV1-ARD protein bound to ATP-agarose in the absence or presence of the indicated concentration of competing ATP or ATP analogs.

nonhydrolyzable analog, AMP-PCP, had an intermediate effect (Figure 3). This strongly correlated with the ability of the reagents to compete TRPV1-ARD binding to ATP-agarose (ATPγS ~ ATP > AMP-PCP; Figure 3D). In the crystal structure, K160 contacts the β-γ-bridging oxygen of ATP. This oxygen is replaced by a methylene group in AMP-PCP, likely explaining its reduced affinity. Overall, the data support the idea that the effect of ATP on TRPV1 tachyphylaxis is mediated through a direct interaction with the TRPV1-ARD, rather than indirectly through cellular metabolism.

TRPV1 channels with mutations in the ATP-binding site—K155A, K160A, or Y199A/Q202A—showed little tachyphylaxis even in the absence of ATP, while the two negative control mutants—R181A and K265A—had essentially wild-type behavior (Figures 4A and 4B). To describe and compare tachyphylaxis quantitatively we measured the maximal current amplitude evoked by repeated

3 min applications of 200 nM capsaicin (Figure 4B). The prolonged first capsaicin application (8 min) ensured that we had reached maximal current in the first application, and thereby maximized the tachyphylaxis response, even for the K155A, K160A, or Y199A/Q202A mutants, which exhibited slow activation kinetics for the first capsaicin application (Figure 4A). Interestingly, the slow activation of the mutants was ATP-independent. The Y199A/Q202A mutant also had a slow deactivation after capsaicin washout (Figure 4A).

We and others have observed that the amount of TRPV1 desensitization is at least in part related to initial current densities (e.g., Bhave et al., 2002 and Mohapatra and Nau, 2003). Initial current densities reflect the amount of calcium that enters the cell, activating the desensitization process. To rule out the possibility that the lack of tachyphylaxis in the TRPV1 mutants is due to either poor cell surface expression (overall expression levels of wild-type
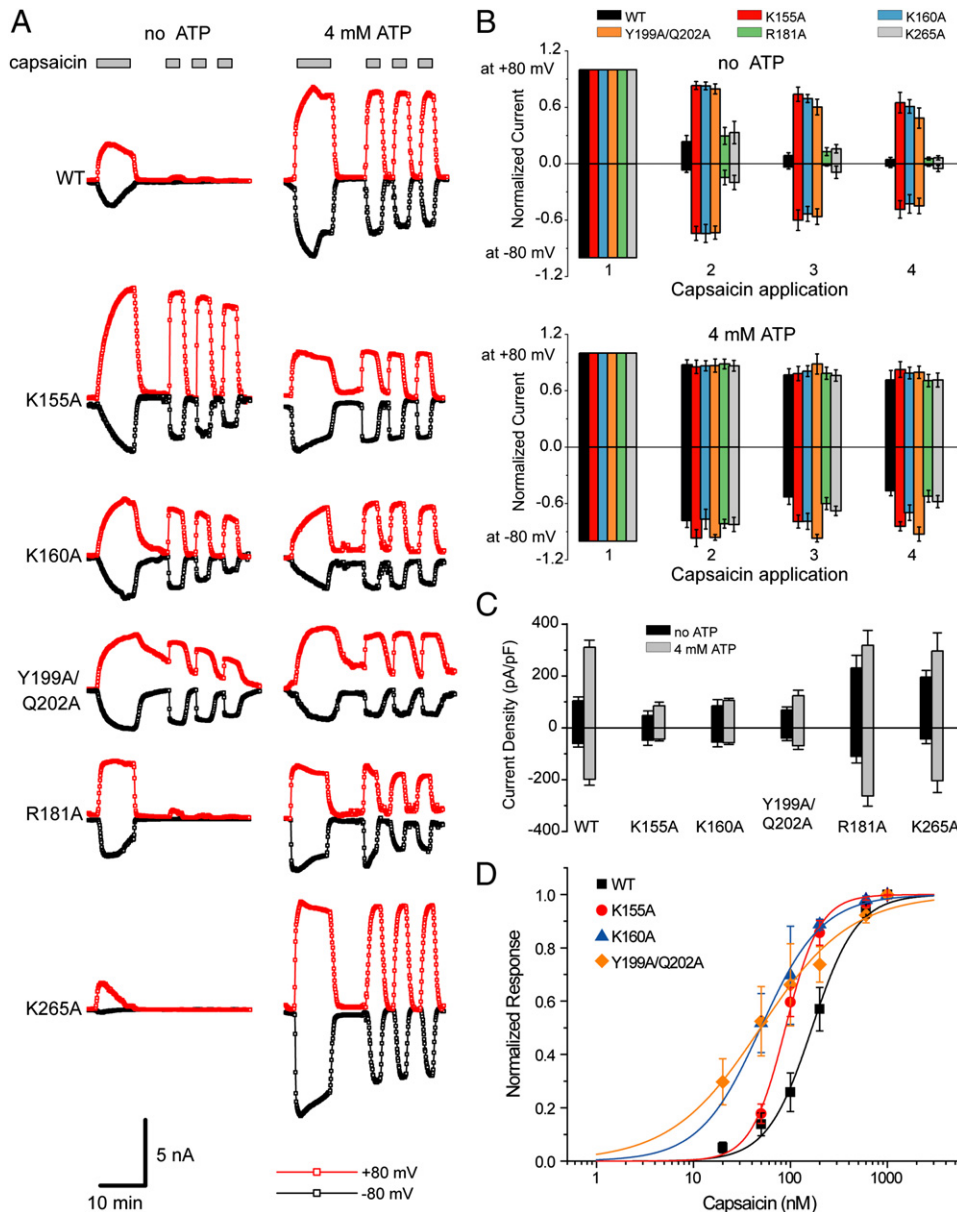
Figure 4. Mutations within the ATP-Binding Site Eliminate Tachyphylaxis in the Absence of ATP

(A) Sample inward and outward current traces from Sf21 insect cells expressing either wild-type or mutant TRPV1 and stimulated with repeated applications of 200 nM capsaicin (gray bars). On the left are representative traces from cells recorded in the absence of ATP. For the cells recorded in the presence of ATP (right), 4 mM ATP was added to the pipette (intracellular) solution and is therefore present throughout the recording. Cells were first stimulated with capsaicin for 8 min followed by 8 min washout, and each subsequent capsaicin stimulation and washout was 3 min. The +80 mV (red) and −80 mV (black) currents are shown, extracted from 1500 ms voltage ramps.

(B and C) Mean current amplitudes for successive capsaicin applications, normalized to the current amplitudes obtained on the first application, for cells measured in the absence (top) or presence (bottom) of ATP (B); and mean current density of the maximal response to the first capsaicin application normalized to the cell capacitance (C). The values were calculated from current amplitudes at −80mV (negative scale) and +80 mV (positive scale) measured in experiments as shown in (A). Bars represent mean ± SEM (n = 11/5, 7/7, 9/8, 8/5, 5/7, 7/5 for WT, K155A, K160A, Y199A/Q202A, R181A, and K265A without or with ATP, respectively).

(D) Capsaicin dose-response curves for TRPV1 and mutants in the absence of ATP. Responses to each dose of capsaicin were normalized to the maximum response measured in each cell, and plotted against the capsaicin concentration. The lines represent the fit of the data to the Hill equation. EC_{50} values and Hill coefficients (n) were as follows: 167 ± 9 nM, n = 1.9 for wild-type; 89 ± 3 nM, n = 2.5 for K155A; 49.4 ± 0.9 nM, n = 1.4 for K160A; and 45 ± 5 nM, n = 0.9 for Y199A/Q202A. Curves were obtained from seven cells each. Error bars are SEM.
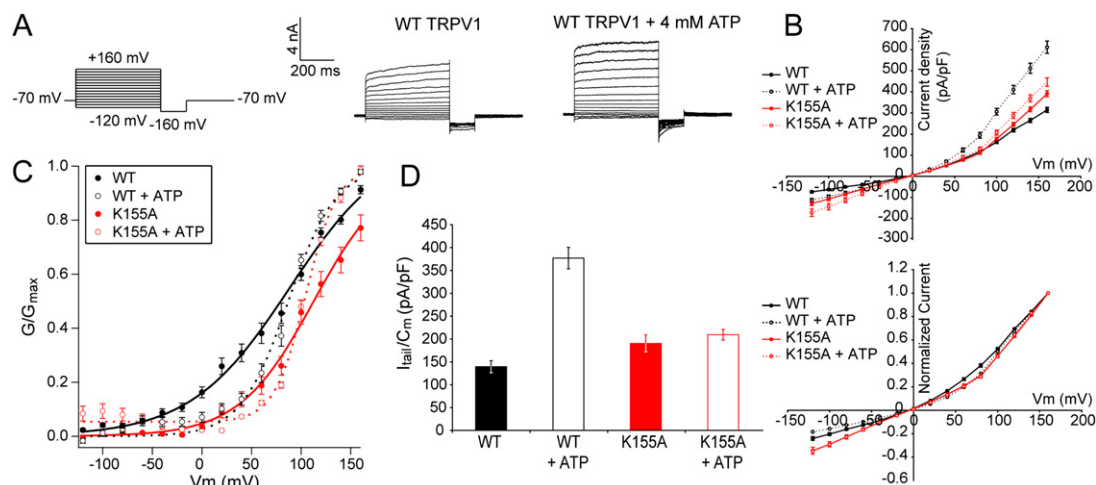
Figure 5. ATP Does Not Shift the Voltage Dependence of Wild-Type TRPV1 or the K155A Mutant

(A) Sample whole-cell current traces from wild-type TRPV1 (WT) expressed in Sf21 insect cells in response to the indicated voltage protocol after reaching steady state to the application of 200 nM capsaicin, without (middle) or with 4 mM ATP (right) in the pipette solution.

(B) Current density (top) and normalized current (bottom) versus voltage for the aggregate data.

(C) Activation curves of wild-type (black) and K155A (red) in the presence (open circles) and absence (filled circles) of 4 mM ATP calculated from the tail currents measured during the first milliseconds after the step to −160 mV in experiments as shown in (A) and normalized to the maximal tail current. Lines represent the Boltzmann function fit to the data.

(D) Average maximum tail current amplitude from wild-type and K155A TRPV1 activated by 200 nM capsaicin. For (B), (C), and (D), values are average ± SEM (n = 7).

and mutant TRPV1 proteins were indistinguishable by western blot; Figure S4) or smaller current amplitudes, we measured the maximal current density of the first capsaicin response in the presence or absence of ATP (Figure 4C). All mutant channels had initial current densities similar to or greater than wild-type TRPV1 in the absence of ATP and similar current voltage relationships (Figure S2C), thereby ruling out an effect of the initial current density on tachyphylaxis. Interestingly, in the presence of 4 mM ATP (and likewise for 4 mM ATPγS and 4 mM AMP-PCP; Figure 3C), wild-type TRPV1 was significantly sensitized with an inward current density about 3-fold higher than in the absence of ATP, while the K155A, K160A, or Y199A/Q202A mutant channels show little sensitization. Capsaicin dose-response curves obtained by applying steps of increasing concentrations of capsaicin in the absence of ATP also confirm that the lack of tachyphylaxis shown by the TRPV1 mutants is not due to impaired capsaicin sensitivity (Figure 4D). In fact, the mutant channels were slightly more sensitive to capsaicin than the wild-type channel.

Voets and colleagues showed that both temperature and capsaicin shift the voltage dependence of TRPV1 activation, allowing TRPV1 to open at more negative membrane potentials (Voets et al., 2004). In order to determine whether ATP also shifts the voltage dependence of activation, activation curves under steady-state capsaicin stimulation were determined from tail currents at −160 mV in a voltage step protocol for wild-type and K155A TRPV1 in the presence or absence of ATP (Figure 5). Wild-type TRPV1 did not show any significant shift in the midpoint

of voltage activation ($V_{1/2}$) in the presence of 4 mM ATP ($V_{1/2}$ 77.5 ± 1.9 mV and 76.2 ± 3.5 mV with and without ATP, respectively. n = 7). The $V_{1/2}$ of K155A was also unaffected by ATP (106 ± 1.9 mV and 113 ± 8.4 mV with and without ATP, respectively. n = 7). However, the addition of ATP significantly increased the maximal tail current amplitude of wild-type TRPV1, while the K155A tail current magnitude was unaffected (Figure 5D). Addition of ATP, therefore, results in increased maximal conductance but does not change the voltage dependence properties of TRPV1. The increased conductance could be due to a combination of several factors, including an increased probability for the channel to be in an open state, an increase in number of channels available for activation, or an increase of individual channel conductance.

In summary, our electrophysiology results demonstrate that the residues within the ATP-binding site in TRPV1-ARD are important for TRPV1 channel regulation, since mutations in the ATP-binding site impair tachyphylaxis and ATP-mediated sensitization. These observations are inconsistent with a simple model where ATP binding to TRPV1 sensitizes the channel and reduces tachyphylaxis. In that case, the TRPV1 mutants would show tachyphylaxis both in the absence and presence of ATP, contrary to what we observed. However, our results can readily be explained if we hypothesize an additional inhibitory ligand which inactivates the channel. In this model, two ligands, one sensitizing and one inhibitory, compete for the same binding site, and the mutations impairing binding of the sensitizing ATP ligand also impair TRPV1 inhibition by the other inhibitory ligand. By impairing interactions
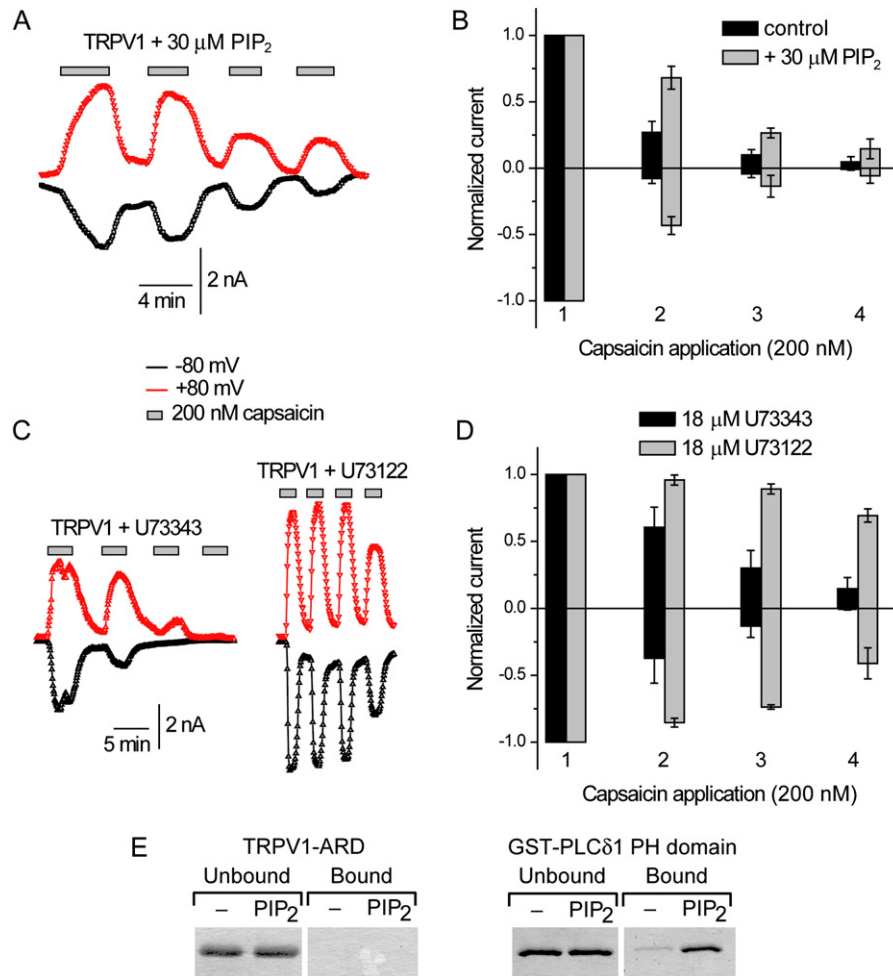
Figure 6. Preventing PIP$_2$ Depletion Reduces TRPV1 Tachyphylaxis

(A) Recording from an insect cell expressing WT-TRPV1, showing that 30 μM PIP$_2$ in the recording pipette partially reduces tachyphylaxis.

(B) Aggregate data from four successive capsaicin applications on several cells with (gray bars) or without PIP$_2$ (black bars) in the recording pipette (n = 5 and 8, respectively). Error bars are SEM.

(C) Recording from a TRPV1-expressing insect cell in the presence of 18 μM control compound U73343 (left) or 18 μM PLC inhibitor U73122 (right) in the recording pipette.

(D) Aggregate data from four successive capsaicin applications in the presence of U73122 (gray bars) or U73343 (black bars), (n = 4 and 5 cells, respectively). Error bars are SEM.

(E) TRPV1-ARD does not bind PIP$_2$-containing artificial liposomes. TRPV1-ARD did not coprecipitate with liposomes containing PIP$_2$ (left), while under the same conditions, the PH domain of PLCδ1, fused to GST, was precipitated with liposomes containing PIP$_2$ (right).

with both the sensitizing and inhibitory ligand, the mutants lack tachyphylaxis.

PIP$_2$ Also Prevents TRPV1 Tachyphylaxis

Several reports suggest that TRPV1 is regulated by PIP$_2$, although there are discrepancies about its regulatory role. Two groups reported that PIP$_2$ upregulates TRPV1 and that PIP$_2$ depletion desensitizes the channel in mammalian cells (Liu et al., 2005; Stein et al., 2006), while Prescott and Julius have provided evidence using a *Xenopus leavis* oocyte system suggesting that PIP$_2$ is an inhibitor of TRPV1 (Prescott and Julius, 2003). There is evidence supporting an indirect role for ATP in replenishing PIP$_2$ in

HEK293 cells (Liu et al., 2005). We therefore decided to test whether PIP$_2$ levels also modulate TRPV1 function in insect cells using electrophysiology; that is, whether ATP may regulate TRPV1 by multiple mechanisms.

When 30 μM PIP$_2$ was added to the intracellular pipette solution to reduce PIP$_2$ depletion, we observed a partial reduction in tachyphylaxis to repeated capsaicin applications in the absence of ATP (Figures 6A and 6B). This indicates that PIP$_2$ sensitizes TRPV1 in insect cells and suggests that PIP$_2$ depletion in the absence of ATP contributes to the observed tachyphylaxis. In a second set of experiments, we investigated channel behavior in the presence of phospholipase C (PLC) inhibitor U73122

(Smith et al., 1990) to prevent PIP_2 degradation by endogenous phospholipases or its inactive analog U73343. Addition of 18 μM U73122 inhibitor to the intracellular pipette solution nearly completely eliminated tachyphylaxis in TRPV1-expressing insect cells, whereas cells treated with the control U73343 compound (18 μM) showed wild-type behavior (Figures 6C and 6D). These two experiments indicate that the presence of PIP_2 prevents TRPV1 tachyphylaxis in insect cells, consistent with evidence obtained with TRPV1 expressed in HEK293 cells (Liu et al., 2005).

Of note, PIP_2 has been shown to physically interact with a C-terminal fragment of TRPV1 (Kwon et al., 2007). Because our electrophysiology data demonstrate that ATP and PIP_2 can both prevent TRPV1 tachyphylaxis, we aimed to determine whether the TRPV1-ARD can also bind to phosphoinositides in vitro. Under conditions where the phospholipase C δ1 PH domain binds to artificial liposomes containing PIP_2, no binding of the TRPV1-ARD is observed (Figure 6E). However, in cells, the colocalization of TRPV1 and PIP_2 at the cell membrane results in a higher effective concentration of PIP_2, and we cannot completely rule out that PIP_2 binds the isolated TRPV1-ARD with an affinity too weak to detect in our assays but still physiologically relevant.

Role of CaM in TRPV1 Desensitization and Tachyphylaxis

Our experiments indicate that ATP and PIP_2 sensitize TRPV1 in agreement with previously published data (Liu et al., 2005; Stein et al., 2006). We next aimed to identify the inhibitory ligand that interacts with the TRPV1-ARD to cause tachyphylaxis. A good candidate for this inhibitor is CaM. It has been reported that Ca^{2+}-CaM binds to peptides from the N-terminal region of TRPV1 and that residues 189–222 are important determinants for binding (Rosenbaum et al., 2004). These residues form finger 2 and inner and outer helices 3 of the TRPV1-ARD (Figure 1). The Ca^{2+}-CaM / TRPV1 interaction was found to reduce channel open probability (Rosenbaum et al., 2004). It is also known that TRPV1 desensitization is a calcium-dependent process, as its observation by electrophysiology requires calcium in the recording solution (Numazaki et al., 2003).

In order to test the role of CaM in TRPV1 tachyphylaxis, we aimed to prevent CaM association with TRPV1 in cells and assay, using electrophysiology, for changes in capsaicin-evoked responses. We used a mouse monoclonal anti-CaM antibody (CaM85) to sequester CaM in TRPV1-transfected HEK293 cells. Of note, Sf21 CaM (accession number DY793505; Deng et al., 2006) and rat CaM are 98% identical (human and rat CaM are 100% identical) with the few differences localized at the C terminus. It is therefore very likely that the rat TRPV1 protein interacts with insect CaM when expressed in insect cells. However, since most anti-CaM antibodies, including CaM85, target the mammalian CaM C terminus, we used HEK293 cells rather than insect cells for these experiments. When added to the intracellular pipette solution, the anti-CaM antibody reduced both acute desensitization and tachyphylaxis of the TRPV1-mediated inward currents, whereas an isotype-matched control antibody had no effect on the TRPV1 response (Figures 7A and 7B). Interestingly, addition of CaM85 also resulted in slower TRPV1 activation in the second, third, and fourth capsaicin applications (Figure 7A), similar to that observed for the K155A, K160A and Y199A/Q202A mutants (Figure 4A). Reducing the CaM levels in TRPV1-expressing HEK293 cells using RNAi produced similar results, although the amplitude of the effect was smaller, likely because the CaM knock down was only partial (Figure S5). Our data therefore support the hypothesis that CaM is the inhibitory molecule causing TRPV1 tachyphylaxis.

CaM Interacts with the TRPV1-ARD

Our electrophysiology data show that CaM is necessary for TRPV1 tachyphylaxis. To determine the extent of the interplay between ATP and CaM in regulating TRPV1 sensitivity, we tested whether the TRPV1-ARD also binds CaM using size exclusion chromatography. Purified CaM and TRPV1-ARD were incubated with Ca^{2+}, EGTA, or Ca^{2+} plus ATP and analyzed by size exclusion chromatography at salt concentrations corresponding to physiological osmolarity (Figures 7C–7E). In the presence of 0.16 mM Ca^{2+}, the proteins eluted at a higher apparent molecular weight, indicating complex formation (Figure 7C) (Sf21 CaM also forms the same complex [Figure S6B]). The observed shift in peak elution volume and analysis of eluted fractions by SDS-polyacrylamide gel electrophoresis (Figure S6A) are both consistent with formation of a 1:1 stoichiometric complex. This complex was Ca^{2+}-dependent (Figure 7D) and dissociated in the presence of ATP (Figure 7E), suggesting that CaM and ATP bind the same region on the TRPV1-ARD. Note that we determined that 5 mM ATP and 2 mM Ca^{2+} corresponds to 3.2 mM free ATP and 0.16 mM free Ca^{2+} in our size exclusion chromatography buffer, using MaxChelator (Patton et al., 2004). TRPV1-ARD failed to shift with CaM1234, a CaM mutant that no longer binds Ca^{2+} (Keen et al., 1999), by size exclusion chromatography (Figure S6C), further demonstrating the Ca^{2+}-dependence of the complex. The homologous TRPV2-ARD, which did not precipitate with ATP-agarose, similarly did not associate with CaM (Figure S6D).

Furthermore, the TRPV1-ARD mutants K155A and K160A, which no longer bind ATP, did not interact with CaM in our size exclusion chromatography assay (Figures 7F and 7G), emphasizing that the binding surface on TRPV1-ARD is at least partially shared by both ligands. The TRPV1-ARD Y199A/Q202A mutant, where residues important for interactions with the adenine moiety of ATP were mutated, formed a complex with CaM that eluted earlier than the complex with wild-type TRPV1-ARD (Figure 7G). Coomassie-stained gels indicated that the complex still had a 1:1 stoichiometric ratio (data not shown), suggesting that the different elution properties may be
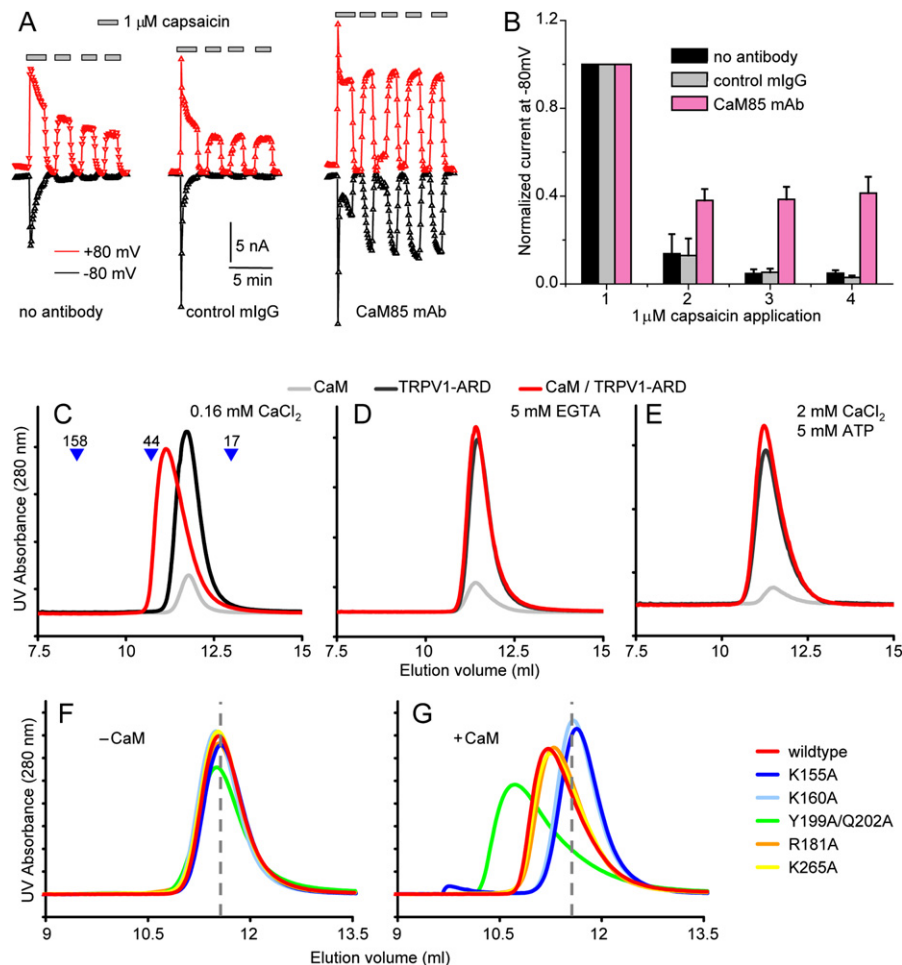
Figure 7. An Anti-CaM Antibody Prevents Tachyphylaxis of TRPV1 in HEK293 Cells, and CaM Forms a Ca^{2+}-Dependent Complex with TRPV1-ARD

(A) Sample whole-cell patch-clamp recordings of TRPV1-expressing HEK293 cells. The monoclonal anti-CaM antibody CaM85 (2 µg/mL) inhibits TRPV1 tachyphylaxis when added to the intracellular pipette solution (compare traces on the left and right), whereas 2 µg/mL isotype-matched control antibody has no effect (middle). Recordings started ~5 min after break-in to allow the cells to stabilize and the antibodies to diffuse through the cells. The +80 mV (red) and –80 mV (black) currents are shown, extracted from 1500 ms voltage ramps.

(B) Normalized amplitudes of the inward currents (at –80 mV) recorded from HEK293 cells in the presence or absence of antibody (n = 3, 3, and 5 cells for wild-type, control, and CaM85 antibodies, respectively). Error bars are SEM.

(C–E) When mixed together in the presence of 0.16 mM Ca^{2+}, CaM (25.5 nmol) and TRPV1-ARD (25.5 nmol) elute as a higher molecular weight complex from a size exclusion chromatography column (C). This complex is disrupted by replacement of Ca^{2+} with 5 mM of the chelating agent EGTA (D), or by addition of 5 mM ATP with 2 mM Ca^{2+} ([E], free ATP = 3.2 mM, free Ca^{2+} = 0.16 mM). Elution volumes of molecular weight standards (in kDa) are indicated in panel (C). Shown are representative traces from three experiments.

(F and G) Wild-type and mutant TRPV1-ARDs (12.5 nmol) were injected on a size exclusion chromatography column alone (F), or together with CaM (12.5 nmol) (G), all in the presence of 2 mM CaCl$_2$. The vertical dashed line indicates the peak elution volume of wild-type TRPV1-ARD alone for comparison between the graphs. Shown are representative traces from two experiments.

due to an altered conformation or binding constant, or higher order (e.g., 2:2) complex. Full-length TRPV1 Y199A/Q202A channels also had unique characteristics in electrophysiology experiments presented above (Figure 4). Overall, the electrophysiology and biochemical data clearly indicate that TRPV1-ARD binds CaM, that the interface is at least partially shared with triphosphate nucleotides, and that this interaction is crucial to inactivation of the channel following repeated stimulation.

DISCUSSION

Following activation by pain-inducing stimuli, TRPV1 is inactivated by a Ca^{2+}-dependent mechanism. This desensitization of the channel prevents continued perception of the stimulus, and has led, at first glance paradoxically, to the investigation of TRPV1 agonists as analgesics for the treatment of chronic pain. Calmodulin has been identified as a component of the inactivation machinery, although

discrepancies have existed as to its binding site on TRPV1 and possible interplay with other intracellular ligands.

Our studies identify a multiligand-binding site in the TRPV1-ARD. Disruption of this site by mutagenesis, guided by crystal structures with ATP occupying the binding site, revealed two important features. First, these mutations eliminated tachyphylaxis, suggesting that a channel inhibitor, identified as Ca^{2+}-CaM, no longer bound. Second, unlike wild-type TRPV1, these mutants were not sensitized in the presence of ATP, suggesting that ATP binds and sensitizes wild-type TRPV1, but no longer bound the mutants. Figure 8 illustrates the model for the modulation of TRPV1 sensitivity that emerges from our data. In resting cells, the sensitizer concentration is high, and the intracellular calcium concentration is low. Under these conditions, the TRPV1-ARD is bound to a sensitizer, likely ATP, and the channel is sensitized. Upon TRPV1 activation, Ca^{2+} influx activates CaM, and Ca^{2+}-CaM replaces the sensitizer on TRPV1 and generates an inactivated state of the channel. Although some aspects remain hypothetical, the model incorporates our data and much of the literature on TRPV1 regulation by ATP, PIP_2 and CaM, and provides a basis for future experiments. Below we summarize the evidence in support of this model.

Calmodulin is clearly implicated as the inhibitory ligand. The use of CaM as a Ca^{2+} sensor to either facilitate or inhibit activity is a common feature of numerous channels, including other TRP family members (Niemeyer, 2005; Saimi and Kung, 2002; Zhu, 2005). Our data show that CaM binds the TRPV1-ARD only in the presence of Ca^{2+} and that CaM sequestration prevents tachyphylaxis, as do mutations that alter Ca^{2+}-CaM/TRPV1-ARD complex formation. Hence, when TRPV1 channels open, Ca^{2+} enters the cell and binds CaM, and Ca^{2+}-CaM engages the ARD to close the channel. Previous studies have implicated CaM binding to N- and C-terminal regions of TRPV1. CaM was found to interact with TRPV1 in a Ca^{2+}-independent manner (Rosenbaum et al., 2004), and binding of CaM to a C-terminal region of TRPV1 (residues 767–800) was Ca^{2+}-independent (Numazaki et al., 2003). A Ca^{2+}-dependent interaction was mapped to residues 189–222 using isolated peptides (Rosenbaum et al., 2004). This last observation agrees with our data using the folded TRPV1-ARD, since we implicate residues within and adjacent to this segment in the tertiary structure as important for the interaction with CaM. In aggregate, these findings suggest that CaM may be anchored in a Ca^{2+}-independent manner to the C terminus such that, upon Ca^{2+} entry after channel opening, Ca^{2+}-CaM crosslinks the N and C termini of TRPV1 and inactivates the channel.

ATP can bind the TRPV1-ARD and sensitize the channel, generating larger currents in response to capsaicin application. Our results with nonhydrolyzable ATP analogs (Figure 3) strongly support that direct ATP binding sensitizes TRPV1. Other ion channels are regulated by ATP, tying channel function to metabolism. In particular, K_{ATP} channels, which are widely expressed in contractile
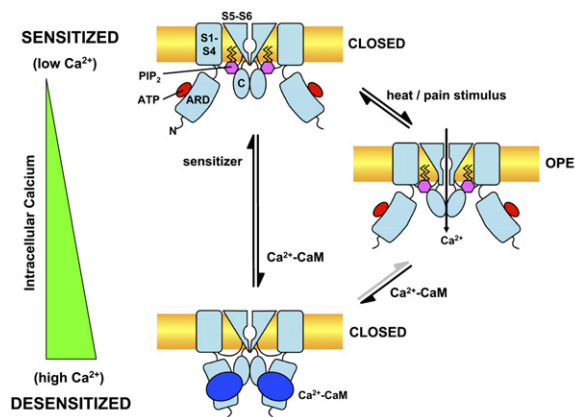

Figure 8. Model of Modulatory Interactions with the TRPV1-ARD Ligand-Binding Site
In the sensitized state, the N-terminal TRPV1-ARD is bound to ATP, and PIP_2 is bound to a C-terminal site. Intracellular calcium influx causes release of ATP and degradation of PIP_2. Ca^{2+}-CaM now binds the exposed TRPV1-ARD, generating an inactive, desensitized conformation of the channel.

tissues, the brain and pancreatic β cells, modulate activity based on intracellular ADP/ATP levels to dampen cell excitability during metabolic stress or promote insulin release, depending on the cell type (Nichols, 2006). However, ATP binding to TRPV1 is inhibited by divalent cations, and hence its role in vivo, where most ATP is chelated by Mg^{2+}, is uncertain. Still, the cellular concentration of unchelated ATP ranges from 0.3–0.7 mM ((Taylor et al., 1991) and references therein). Therefore, ATP binding to the ARD suggests an elegant desensitization mechanism: in a resting cell, ATP is bound and the channel sensitized, but after channel opening, Ca^{2+} and Mg^{2+} flow inward and chelate and release the ATP from TRPV1-ARD. The binding site is now accessible to interact with Ca^{2+}-CaM.

ATP has also been shown to act indirectly via phosphoryl transfer to replenish PIP_2 (Liu et al., 2005), and we and others have observed that PIP_2 sensitizes TRPV1 (Liu et al., 2005; Stein et al., 2006). PIP_2 binds the TRPV1 C-terminal region and, analogous to ATP binding at the TRPV1-ARD, PIP_2 competes with CaM for binding to the TRPV1 C terminus (Kwon et al., 2007). Another report highlights the importance of the C-terminal TRP box, at least in TRPM8, TRPM5, and TRPV5, in mediating the effects of PIP_2 (Rohács et al., 2005). An appealing model is that in resting cells, which have high PIP_2, TRPV1 is bound to PIP_2, likely through its C terminus, and sensitized. Following channel opening, Ca^{2+} enters and activates phospholipase C, depleting the PIP_2 pool. Ca^{2+}-CaM now binds the TRPV1-ARD (our work and Rosenbaum et al., 2004) and TRPV1-C-terminus (Kwon et al., 2007; Numazaki et al., 2003) and stabilizes an inactivated state of the channel.

A recent paper describes a role for PIP_2 in regulating the trafficking of TRPV1 to the plasma membrane (Stein et al., 2006). However, we did not observe changes in

membrane capacitance over the course of our whole-cell patch-clamp electrophysiology experiments. It is therefore unlikely that the current changes we observed are due to a change in the number of channels localized at the plasma membrane, although such trafficking may provide an additional layer of TRPV1 regulation in vivo.

Ion channels are often regulated by phosphorylation. There is growing evidence that Ca^{2+}-dependent dephosphorylation of the cytosolic N terminus of TRPV1 is implicated in channel desensitization (see Tominaga and Tominaga, 2005 for a review). In particular, protein kinase A (PKA) phosphorylates several residues within TRPV1 (Bhave et al., 2002; Mohapatra and Nau, 2003), including S116, which is on inner helix 1 of the TRPV1-ARD, in close proximity to the γ-phosphate of the bound ATP in our structure. Src-dependent phosphorylation of Y200 in human TRPV1 (Y199 in rat TRPV1) has also been observed (Jin et al., 2004). Because S116 and Y199 are located near the binding site in TRPV1-ARD, the negative charges introduced by their phosphorylation could interfere with binding of negatively charged CaM (calculated isoelectric point of 4.1). Although this model requires further investigation, it suggests that phosphorylation could provide another regulatory layer to prevent Ca^{2+}-induced desensitization by preventing interactions with CaM.

The ATP-binding site within the TRPV1-ARD is very well conserved between species, while significant divergence can be found within the TRPV subfamily (Figure S7). TRPV3 shows the highest level of sequence similarity, and it would therefore be interesting to investigate whether ATP and/or CaM play a role in its modulation. In contrast, R115, which interacts with the γ-phosphate of ATP, is replaced by an aspartate (D80) in TRPV2, and this substitution likely explains the inability of TRPV2 to associate with ATP. TRPV4, TRPV5, and TRPV6 also show sequence divergence, and likely do not bind ATP. Deletions within the TRPV6-ARD affect TRPV6 tetramerization (Erler et al., 2004), implicating the TRPV6-ARD in maintaining the structural integrity of the TRPV6 tetramer. Further structural and biochemical studies of the ARDs of different TRPV proteins are needed to determine how they play different roles in TRPV channel function.

We have demonstrated that the TRPV1-ARD modulates channel activity by binding the inhibitory protein ligand calmodulin and by binding a sensitizing small molecule ligand, ATP. This is, to our knowledge, the first example of an ankyrin repeat domain binding a small molecule, expanding the spectrum of functional roles for ankyrin repeats. A model for the Ca^{2+}-dependent desensitization of TRPV1 is now emerging that is consistent with multiple studies and open to further investigation.

EXPERIMENTAL PROCEDURES

Reagents
Capsaicin and capsazepine were purchased from Sigma. All nucleotides were purchased as sodium salts from Sigma except ATPγS (lithium salt, Calbiochem), and stock solutions were prepared to pH ~7.5

with NaOH. Mouse monoclonal anti-calmodulin antibody CaM85 was from Invitrogen, and water soluble DiC_8-PIP_2 from Echelon Bioscience.

Cloning of Expression Vectors
Rat TRPV1 cDNA (provided by Michael Caterina) fragments encoding residues 101–364 (TRPV1-ARD) and 1–838 (full-length) were cloned into the Nde I and Not I sites of pET21-C6H (Jin et al., 2006) and pFastBac-CFlag vectors, respectively. pFastBac-CFlag was generated by ligating a short double-stranded fragment (oligos TCGACACT AGTGACGTCGCGGCCGCTGATTACAAGGATGACGACGATAAGTGA and GGCCTCACTTATCGTCGTCATCCTTGTAATCAGCGGCCGCGA CGTCACTAGTG) in the Sal I and Not I sites of pFastBac1 (Invitrogen). The N604S mutant (Rosenbaum et al., 2002), which is unglycosylated, was used for all experiments in insect cells. Baculovirus stocks were generated and used to infect Sf21 cells as described in the Bac-to-Bac manual (Invitrogen). All mutants were generated by Quick-change mutagenesis (Stratagene), and all clones were verified by DNA sequencing. Refer to Jin et al., 2006 for TRPV2-ARD protein expression and purification.

Expression and Purification of TRPV1-ARD
TRPV1-ARD was expressed in *E. coli* BL21(DE3) cultured in LB and induced at $OD_{600} = 0.5$ with 75 μM IPTG at room temperature for 8–16 hr. Selenomethionine (Se-Met)-substituted TRPV1-ARD was expressed with feedback inhibition of methionine synthesis in fully supplemented M9 minimal media, replacing methionine with Se-Met. Cells expressing TRV1-ARD were resuspended in lysis buffer (50 mM sodium phosphate [pH 7.0], 300 mM NaCl, 20 mM imidazole, 1 mM phenylmethyl-sulfonylfluoride [PMSF], 10 mM β-mercaptoethanol [βME]) with 0.2 mg/ml lysozyme and lysed by sonication. The cleared lysate was loaded onto a Ni-NTA column (Qiagen), washed with lysis buffer, and eluted using a step gradient (60, 100, and 250 mM imidazole). Fractions containing TRPV1-ARD were pooled, concentrated, dialyzed against 20 mM sodium phosphate (pH 7.0), 20 mM NaCl, 2 mM EDTA, 1 mM dithiothreitol (DTT), loaded on a ResourceS column (GE Healthcare), and eluted using a linear gradient of 20–400 mM NaCl. Pure fractions were pooled, buffer-exchanged to 20 mM Tris-HCl (pH 7.0), 100 mM NaCl, 1 mM DTT, and concentrated to 10 mg/ml for crystallization. The Se-Met-substituted protein was purified similarly except that buffers contained 5 rather than 1 mM DTT.

Crystallization of TRPV1-ARD
Crystals were grown by hanging drop vapor diffusion with a 1:1 ratio of protein and reservoir solution in each drop. TRPV1-ARD (crystal form I) crystallized at 20°C with 5% PEG 8000, 0.1 M sodium citrate (pH 5.0), and 5 mM ATP in the reservoir. Crystal form II was obtained at 4°C in 3% PEG 8000, 25–100 mM sodium citrate (pH 4.7–5.0), and 5 mM ATP. All crystals were frozen after cryoprotection in reservoir solution containing 30% glycerol.

Data Collection and Structure Determination
X-ray diffraction data were collected at 100 K. Data on Se-Met-substituted TRPV1-ARD crystal form I were collected at the APS BM8 beamline using an ADSC Q315 CCD detector. TRPV1-ARD native data for both crystal forms were collected on a MicroMax-007 X-ray generator equipped with an R-AXIS IV++ detector (Rigaku/MSC Inc). All data were processed with CrystalClear (Rigaku/MSC Inc) or HKL2000 (Otwinowski and Minor, 1997). Data collection statistics are listed in Table 1. The 3.2 Å structure of TRPV1-ARD crystal form I was determined using a combination of Se-Met MAD phasing (SOLVE and RESOLVE; Terwilliger, 2002) and molecular replacement with MOLREP (Vagin and Teplyakov, 2000) using the TRPV2-ARD structure (Jin et al., 2006). The 2.7 Å TRPV1-ARD crystal form II structure was determined by molecular replacement using the crystal form I structure. Model building was done using COOT (Emsley and Cowtan, 2004) and refinement using REFMAC (Murshudov et al., 1997).

Phasing and refinement statistics are provided in Table 1. The atomic coordinates have been deposited in the Protein Data Bank with the entry codes 2NYJ (crystal form I) and 2PNN (crystal form II).

ATP-Agarose Pull-Downs
Each protein (12.5 μg) was diluted to 900 μl with binding buffer (10 mM Tris [pH 7.5], 50 mM NaCl, 1 mM DTT, 0.15% w/v decyl-β-D-maltopyr-anoside) and incubated with 75 μl ATP-agarose (50% slurry, 11 atom spacer to ribose hydroxyls, Sigma) at 4°C for 2 hr. The agarose beads were washed three times with 1 ml binding buffer, resuspended in sample dye and analyzed by PAGE on Coomassie-stained 12% SDS gels.

Insect and Mammalian Cell Culture
Sf21 insect cells were grown at 27°C in Hink's TNM-FH medium containing 10% (v/v) fetal bovine serum and 0.1% pluronic acid. Cells were passaged to coverslips in the same medium without pluronic acid and infected with the appropriate baculovirus. Currents were recorded 44–52 hr postinfection. HEK 293 cells were transfected with rat TRPV1 subcloned into an EGFP-containing vector pTracer-CMV2 (provided by David Clapham) using lipofectamine 2000 (Invitrogen) according to the manufacturer's instructions. Successfully transfected cells, as visualized by fluorescence LED illumination, were used for current recordings 48–72 hr posttransfection.

Electrophysiology
Currents were recorded at room temperature in the whole-cell patch-clamp configuration using an Axopatch 200B amplifier controlled by a Digidata 1322 and pClamp 9.2 software (Molecular Devices). Data were sampled at 5–10 kHz. Whole-cell capacitance was recorded from the amplifier settings. Voltage ramps (1500 ms) from −100 mV to +100 mV were applied every 5 s from a holding potential of 0 mV. Data were analyzed and displayed with Origin 7.0 (OriginLab Corporation) or Clampfit 9.2 (Axon Instruments). For insect cells, the standard intracellular solution contained (in mM) 140 Na-methanesulfonate, 10 HEPES, 10 EGTA, and 2.5 NaCl; pH was adjusted to 7.2 with NaOH. In some experiments, a Cs-containing intracellular solution was used (in mM) 140 Cs-methanesulfonate, 10 HEPES, 10 EGTA, and 2.5 NaCl; pH was adjusted to 7.2 with CsOH. No difference was observed between the Cs- and Na-containing solutions. The control bath (extra-cellular) solution contained (in mM) 150 Na-gluconate, 10 HEPES, 2 CaCl$_2$, and 10 D-glucose; pH adjusted to 7.2 with NaOH. For recordings from EGFP-positive HEK293 cells, the intracellular Cs-containing solution was used, and standard extracellular solution contained (in mM) 150 NaCl, 5 KCl, 2 CaCl$_2$, 1 MgCl$_2$, 10 D-glucose, and 10 HEPES at pH 7.4 adjusted with NaOH. To obtain the activation curves we used the voltage protocol shown in Figure 5A. Tail currents were measured during the first milliseconds after a step to −160mV and normalized to the maximal tail current.

RNAi
Validated Stealth RNAi DuoPack duplexes targeted to human calmodulin (cat. no. 1293742) and the Stealth RNAi Negative Control LO GC Duplex (cat. no. 12935-200) were purchased from Invitrogen. HEK293 cells were plated in 12-well plates 24 hr prior to transfection with 40 nM Stealth RNAi duplex and 40 nM BLOCK-iT Fluorescent Oligo (Invitrogen) using Lipofectamine 2000 (Invitrogen) at 2 mg/l. After 24 hr, high transfection efficiency was confirmed by visualizing uptake of BLOCK-iT Fluorescent Oligo using fluorescence microscopy, and cells were transfected with TRPV1-pTracerCMV2 as described above. After an additional 48 hr, cells were briefly trypsinized and plated onto 12 mm coverslips, allowed to recover for 1 hr, and assayed electro-physiologically. Calmodulin expression silencing was tested by western blot on cell lysates using anti-calmodulin antibody CaM85 (1:1000 dilution, Zymed). The blot was developed with the Super Signal Western Blot Detection kit (Pierce). A loading control blot was probed with Anti-β-Actin Antibody (1:6000 dilution, Abcam).

Purification of Calmodulin
Human CaM (identical sequence to rat CaM, provided by Andrew Bohm) and *Spodoptera frugiperda* CaM (provided by Philippe Four-nier) were expressed in BL21(DE3), purified essentially as described (Drum et al., 2001) and stored in 10 mM Tris (pH 7.5), 10 mM NaCl, 1 mM DTT. CaM1234 (provided by Joel Hirsch) was expressed in BL21(DE3). Cells were lysed in 50 mM Tris (pH 7.5), 100 mM NaCl, 2 mM EDTA, 0.1% βME, 0.5 mM PMSF, and 0.2 mg/ml lysozyme by freeze-thaw cycles. CaCl$_2$ and NaCl were added to the cleared lysate to final concentrations of 5 mM and 150 mM, respectively, and the ly-sate was heated to 70°C. The cleared lysate was loaded on a S200 16/60 column (GE Healthcare; running buffer 10 mM Tris [pH 7.5], 10 mM NaCl, 1 mM DTT), and CaM1234 containing fractions were further purified on a ResourceQ column (GE Healthcare; buffer 20 mM Tris [pH 7.5], 0.1% βME. 1 mM EGTA, 0.1-1 M NaCl gradient) and a second run on a S200 16/60 column as described above.

TRPV1-ARD / CaM Complex Analysis by Size Exclusion Chromatography
All protein samples were preincubated with an equivalent volume of running buffer (20 mM HEPES [pH 7.4], 140 mM NaCl, 1 mM DTT, plus CaCl$_2$, ATP and/or EGTA as indicated) for 1 hr, followed by sepa-ration on a S75 10/30 column (GE Healthcare) using the same running buffer at 4°C.

PIP$_2$ Binding
To detect PIP$_2$ binding, $\sim$50 μg protein was incubated with biotinylated liposomes (0.02 mM total lipid) with or without PtdIns(4,5)P$_2$ (Echelon Biosciences, Cat. No. Y-0000 and Y-P045) in 1 ml binding buffer (20 mM Tris [pH 7.5], 100 mM NaCl, 1 mM DTT, 0.3% w/v decyl-β-D-mal-topyranoside) for 1 hr at 4°C. Streptavidin-agarose (36 μg; Sigma) was added and the samples incubated a further 1 hr, followed by three washes with 900 μl binding buffer. The beads were resuspended in load dye and analyzed by SDS-PAGE and Coomassie-staining.

Supplemental Data
The Supplemental Data can be found with this article online at http://www.neuron.org/cgi/content/full/54/6/905/DC1/.

REFERENCES

Bhave, G., Zhu, W., Wang, H., Brasier, D.J., Oxford, G.S., and Gereau, R.W.t. (2002). cAMP-dependent protein kinase regulates desensitiza-tion of the capsaicin receptor (VR1) by direct phosphorylation. Neuron *35*, 721–731.

Caterina, M.J., and Julius, D. (2001). The vanilloid receptor: A molecu-lar gateway to the pain pathway. Annu. Rev. Neurosci. *24*, 487–517.

Caterina, M.J., Rosen, T.A., Tominaga, M., Brake, A.J., and Julius, D. (1999). A capsaicin-receptor homologue with a high threshold for nox-ious heat. Nature *398*, 436–441.

Caterina, M.J., Schumacher, M.A., Tominaga, M., Rosen, T.A., Levine, J.D., and Julius, D. (1997). The capsaicin receptor: A heat-activated ion channel in the pain pathway. Nature 389, 816–824.

Deng, Y., Dong, Y., Thodima, V., Clem, R.J., and Passarelli, A.L. (2006). Analysis and functional annotation of expressed sequence tags from the fall armyworm Spodoptera frugiperda. BMC Genomics 7, 264.

Drum, C.L., Shen, Y., Rice, P.A., Bohm, A., and Tang, W.J. (2001). Crystallization and preliminary X-ray study of the edema factor exotoxin adenylyl cyclase domain from Bacillus anthracis in the presence of its activator, calmodulin. Acta Crystallogr. D Biol. Crystallogr. 57, 1881–1884.

Emsley, P., and Cowtan, K. (2004). Coot: Model-building tools for molecular graphics. Acta Crystallogr. D Biol. Crystallogr. 60, 2126–2132.

Erler, I., Hirnet, D., Wissenbach, U., Flockerzi, V., and Niemeyer, B.A. (2004). Ca2+-selective Transient Receptor Potential V Channel Architecture and Function Require a Specific Ankyrin Repeat. J. Biol. Chem. 279, 34456–34463.

Hellwig, N., Albrecht, N., Harteneck, C., Schultz, G., and Schaefer, M. (2005). Homo- and heteromeric assembly of TRPV channel subunits. J. Cell Sci. 118, 917–928.

Jin, X., Morsy, N., Winston, J., Pasricha, P.J., Garrett, K., and Akbarali, H.I. (2004). Modulation of TRPV1 by nonreceptor tyrosine kinase, c-Src kinase. Am. J. Physiol. Cell Physiol. 287, C558–C563.

Jin, X., Touhey, J., and Gaudet, R. (2006). Structure of the N-terminal Ankyrin Repeat Domain of the TRPV2 Ion Channel. J. Biol. Chem. 281, 25006–25010.

Jordt, S.E., and Julius, D. (2002). Molecular basis for species-specific sensitivity to "hot" chili peppers. Cell 108, 421–430.

Jung, J., Lee, S.Y., Hwang, S.W., Cho, H., Shin, J., Kang, Y.S., Kim, S., and Oh, U. (2002). Agonist recognition sites in the cytosolic tails of vanilloid receptor 1. J. Biol. Chem. 277, 44448–44454.

Keen, J.E., Khawaled, R., Farrens, D.L., Neelands, T., Rivard, A., Bond, C.T., Janowsky, A., Fakler, B., Adelman, J.P., and Maylie, J. (1999). Domains Responsible for Constitutive and Ca2+-Dependent Interactions between Calmodulin and Small Conductance Ca2+-Activated Potassium Channels. J. Neurosci. 19, 8830–8838.

Koplas, P.A., Rosenberg, R.L., and Oxford, G.S. (1997). The role of calcium in the desensitization of capsaicin responses in rat dorsal root ganglion neurons. J. Neurosci. 17, 3525–3537.

Kwak, J., Wang, M.H., Hwang, S.W., Kim, T.Y., Lee, S.Y., and Oh, U. (2000). Intracellular ATP increases capsaicin-activated channel activity by interacting with nucleotide-binding domains. J. Neurosci. 20, 8298–8304.

Kwon, Y., Hofmann, T., and Montell, C. (2007). Integration of Phosphoinositide- and Calmodulin-Mediated Regulation of TRPC6. Mol. Cell 25, 491–503.

Liu, B., Zhang, C., and Qin, F. (2005). Functional recovery from desensitization of vanilloid receptor TRPV1 requires resynthesis of phosphatidylinositol 4,5-bisphosphate. J. Neurosci. 25, 4835–4843.

McCleverty, C.J., Koesema, E., Patapoutian, A., Lesley, S.A., and Kreusch, A. (2006). Crystal structure of the human TRPV2 channel ankyrin repeat domain. Protein Sci. 15, 2201–2206.

Mohapatra, D.P., and Nau, C. (2003). Desensitization of capsaicin-activated currents in the vanilloid receptor TRPV1 is decreased by the cyclic AMP-dependent protein kinase pathway. J. Biol. Chem. 278, 50080–50090.

Mosavi, L.K., Cammett, T.J., Desrosiers, D.C., and Peng, Z.Y. (2004). The ankyrin repeat as molecular architecture for protein recognition. Protein Sci. 13, 1435–1448.

Murshudov, G.N., Vagin, A.A., and Dodson, E.J. (1997). Refinement of macromolecular structures by the maximum-likelihood method. Acta Crystallogr. D Biol. Crystallogr. 53, 240–255.

Nichols, C.G. (2006). KATP channels as molecular sensors of cellular metabolism. Nature 440, 470–476.

Niemeyer, B.A. (2005). Structure-function analysis of TRPV channels. Naunyn Schmiedebergs Arch. Pharmacol. 371, 285–294.

Numazaki, M., Tominaga, T., Takeuchi, K., Murayama, N., Toyooka, H., and Tominaga, M. (2003). Structural determinant of TRPV1 desensitization interacts with calmodulin. Proc. Natl. Acad. Sci. USA 100, 8002–8006.

Otwinowski, Z., and Minor, W. (1997). Processing of x-ray diffraction data collected in oscillation mode. Methods Enzymol. 276, 307–326.

Patton, C., Thompson, S., and Epel, D. (2004). Some precautions in using chelators to buffer metals in biological solutions. Cell Calcium 35, 427–431.

Prescott, E.D., and Julius, D. (2003). A modular PIP2 binding site as a determinant of capsaicin receptor sensitivity. Science 300, 1284–1288.

Rohács, T., Lopes, C.M.B., Michailidis, I., and Logothetis, D.E. (2005). PI(4,5)P2 regulates the activation and desensitization of TRPM8 channels through the TRP domain. Nat. Neurosci. 8, 626–634.

Rosenbaum, T., Awaya, M., and Gordon, S.E. (2002). Subunit modification and association in VR1 ion channels. BMC Neurosci. 3, 4.

Rosenbaum, T., Gordon-Shaag, A., Munari, M., and Gordon, S.E. (2004). Ca2+/calmodulin modulates TRPV1 activation by capsaicin. J. Gen. Physiol. 123, 53–62.

Saimi, Y., and Kung, C. (2002). Calmodulin as an ion channel subunit. Annu. Rev. Physiol. 64, 289–311.

Sedgwick, S.G., and Smerdon, S.J. (1999). The ankyrin repeat: A diversity of interactions on a common structural framework. Trends Biochem. Sci. 24, 311–316.

Smith, R.J., Sam, L.M., Justen, J.M., Bundy, G.L., Bala, G.A., and Bleasdale, J.E. (1990). Receptor-coupled signal transduction in human polymorphonuclear neutrophils: Effects of a novel inhibitor of phospholipase C-dependent processes on cell responsiveness. J. Pharmacol. Exp. Ther. 253, 688–697.

Stein, A.T., Ufret-Vincenty, C.A., Hua, L., Santana, L.F., and Gordon, S.E. (2006). Phosphoinositide 3-Kinase Binds to TRPV1 and Mediates NGF-stimulated TRPV1 Trafficking to the Plasma Membrane. J. Gen. Physiol. 128, 509–522.

Taylor, J.S., Vigneron, D.B., Murphy-Boesch, J., Nelson, S.J., Kessler, H.B., Coia, L., Curran, W., and Brown, T.R. (1991). Free magnesium levels in normal human brain and brain tumors: 31P chemical-shift imaging measurements at 1.5 T. Proc. Natl. Acad. Sci. USA 88, 6810–6814.

Terwilliger, T.C. (2002). Automated structure solution, density modification and model building. Acta Crystallogr. D Biol. Crystallogr. 58, 1937–1940.

Tominaga, M., and Tominaga, T. (2005). Structure and function of TRPV1. Pflugers Arch. 451, 143–150.

Tominaga, M., Caterina, M.J., Malmberg, A.B., Rosen, T.A., Gilbert, H., Skinner, K., Raumann, B.E., Basbaum, A.I., and Julius, D. (1998). The cloned capsaicin receptor integrates multiple pain-producing stimuli. Neuron 21, 531–543.

Vagin, A., and Teplyakov, A. (2000). An approach to multi-copy search in molecular replacement. Acta Crystallogr. D Biol. Crystallogr. 56, 1622–1624.

Voets, T., Droogmans, G., Wissenbach, U., Janssens, A., Flockerzi, V., and Nilius, B. (2004). The principle of temperature-dependent gating in cold- and heat-sensitive TRP channels. Nature 430, 748–754.

Walker, J.E., Saraste, M., Runswick, M.J., and Gay, N.J. (1982). Distantly related sequences in the alpha- and beta-subunits of ATP synthase, myosin, kinases and other ATP-requiring enzymes and a common nucleotide binding fold. EMBO J. 1, 945–951.

Zhu, M.X. (2005). Multiple roles of calmodulin and other Ca(2+)-binding proteins in the functional regulation of TRP channels. Pflugers Arch. 451, 105–115.